

Quantum dot lasers based on a stacked and strain-compensated active region grown by metal-organic chemical vapor deposition

N. Nuntawong, Y. C. Xin, S. Birudavolu, P. S. Wong, S. Huang, C. P. Hains, and D. L. Huffaker^{a)}

Center for High Technology Materials, University of New Mexico, 1313 Goddard SE, Albuquerque, New Mexico 87106

(Received 15 December 2004; accepted 28 March 2005; published online 6 May 2005)

We demonstrate an InAs/GaAs quantum dot (QD) laser based on a strain-compensated, three-stack active region. Each layer of the stacked QD active region contains a thin GaP ($\Delta a_o = -3.8\%$) tensile layer embedded in a GaAs matrix to partially compensate the compressive strain of the InAs ($\Delta a_o = 7\%$) QD layer. The optimized GaP thickness is ~ 4 MLs and results in a 36% reduction of compressive strain in our device structure. Atomic force microscope images, room-temperature photoluminescence, and x-ray diffraction confirm that strain compensation improves both structural and optical device properties. Room-temperature ground state lasing at $\lambda = 1.249 \mu\text{m}$, $J_{\text{th}} = 550 \text{ A/cm}^2$ has been demonstrated. © 2005 American Institute of Physics.

[DOI: 10.1063/1.1926413]

GaAs-based quantum dot (QD) lasers operating between 1.25 and 1.65 μm continue to intrigue researchers with the potential benefits of zero dimensionality. While the QD active region has low gain at the ground-state transition, stacking the QD layers has been shown to increase ground-state modal gain¹⁻⁶ resulting in ground-state lasing and larger T_o . The growth of QDs and stacked QDs for long wavelength emission using metal-organic chemical vapor deposition (MOCVD) has been difficult due to the high density of relaxed defect clusters that form with increased strain and complicated surface environment.^{7,8} Only recently has ground-state lasing at $\lambda > 1.24 \mu\text{m}$ from MOCVD-grown stacked QDs been demonstrated.⁴⁻⁶ Two approaches have been successful to date. Kim *et al.* has embedded the QDs in an InGaP barrier,⁴ which results in high $T_o = 210 \text{ K}$ and $J_{\text{th}} = 200 \text{ A/cm}^2$ at $\lambda = 1.28 \mu\text{m}$. Kaiander *et al.*⁵ and Tatebayashi *et al.*⁶ have employed annealing steps that remove defect clusters and result in a low transparency current density of 7.2 A/cm² per QD layer at $\lambda = 1.245 \mu\text{m}$.

In our work, we combine two methods to reduce defect propagation in the stacked active region. An AsH₃⁷ pause reduces the defect density at each layer and a GaP tensile layer is inserted within the stacked structure to partially compensate the compressive strain of the QDs. We have previously reported improved crystallinity using InGaP strain-compensation (SC) layers, however, the InGaP layers can lead to In segregation and hexagonal material at the InGaP/GaAs interface.¹¹ The use of InGaP and InGaAsP SC layers has been demonstrated in multiple strained quantum wells lasers.^{9,10} Recently, (In)GaP^{11,12} and GaNAs^{13,14} have been reported in stacked QD structures to improve both crystalline quality and optical properties. However, lasing from SC QD structures has not yet been demonstrated.

In this article, we describe the GaP SC layer optimization and resulting QD laser characteristics. Three sets of samples are analyzed. First, a series of five stacks with varied GaP thickness is evaluated to optimize the SC layer. Second, a set of samples with a varied number of stacks is evaluated

both with and without the GaP SC layers to analyze the progression of strain. These samples are characterized using atomic force microscope (AFM), x-ray diffraction (XRD), and photoluminescence (PL). Finally, the three-stack laser structure and its characteristics are described.

The sample growth is described in detail elsewhere.^{7,11} All active regions consist of a 5 ML In_{0.15}Ga_{0.85}As buffer, 3 ML InAs QDs, and a 25 ML In_{0.15}Ga_{0.85}As cap. A post nucleation AsH₃ pause⁷ is used after the growth of each QD layer to reduce the defect density. The stacked QD layers are separated by an 8 nm GaAs barrier sandwiching a thin (2–8 ML) GaP layer resulting in a lattice mismatch to the GaAs matrix of 3.8%. The laser structures are grown on *n*-type substrates followed by 300 nm GaAs *n*⁺ doped, a 0.8 μm *n*-Al_{0.7}GaAs ($n \sim 1 \times 10^{17} \text{ cm}^{-3}$) lower clad, 110 nm GaAs waveguide embedding the active region, and a 0.8 μm *p*-Al_{0.7}GaAs ($p \sim 1 \times 10^{17} \text{ cm}^{-3}$) upper clad. The structures are terminated with a 50 nm GaAs *n*⁺ layer.¹⁵

Figure 1 shows room-temperature photoluminescence (RTPL) from a series of five-stack structures with varied GaP layer thickness including 2, 4, 6, and 8 MLs. Several trends can be noted. Overall, the PL intensity is more than one order of magnitude higher with GaP SC layers than without. As the thickness of a GaP layer increases, we observe a blueshift from 1.33 to 1.25 μm due to a 9% reduction in QD size

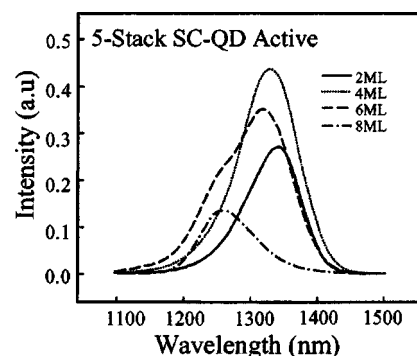


FIG. 1. Room-temperature PL from five-stack samples with 2, 4, 6, and 8 MLs of GaP SC layer.

^{a)}Electronic mail: huffaker@chtm.unm.edu

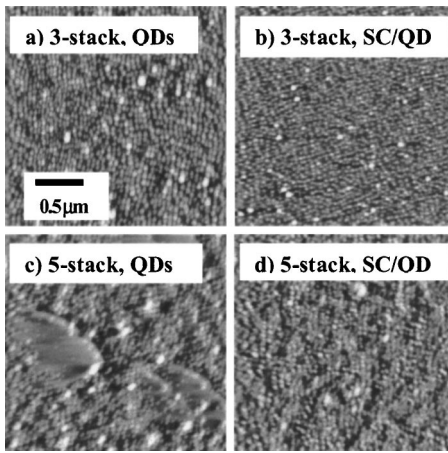


FIG. 2. (Color online) AFM images ($2\ \mu\text{m} \times 2\ \mu\text{m}$) showing the top layer of a three stack (a) without SC, and (b) with SC and a five stack (c) without SC, and (d) with SC.

driven by the increased tensile strain. The PL intensity increases with a GaP layer thickness from 2 to 4 MLs then decreases for thicknesses of 6 and 8 MLs. The decrease in PL intensity associated with the thicker GaP layers can be attributed to partial relaxation of the SC layer and dislocations in the structure. The critical thickness of the embedded GaP layer is expected to be much lower than the value reported at 12 MLs¹⁶ for GaP on GaAs due to the existing strain from QD region. The total average strain values for each sample were obtained from XRD spectra (not shown) by¹¹

$$\langle \varepsilon_{\perp} \rangle = \frac{\sin \theta_B}{\sin(\theta_B + \Delta\theta)} - 1, \quad (1)$$

where θ_B is the Bragg angle of the GaAs substrate, $\Delta\theta$ is the separation between zero-order peak and GaAs peak. This calculation indicates total strain changes from 0.014 897 without SC to 0.009 550 with 4 MLs GaP (36% reduction). Details of XRD characterization is described in our previous work.¹¹ A simple summation of strain using Eqs. (2) and (3) confirms the 36% strain reduction with the presence of GaP layers:

$$\langle \varepsilon_{\perp} \rangle = \frac{\sum_i (\varepsilon_{\perp})_i \cdot t_i}{\sum_i t_i}, \quad (2)$$

$$\varepsilon_{\perp} = \frac{a_i - a_{\text{GaAs}}}{a_{\text{GaAs}}}, \quad (3)$$

where ε_{\perp} and t are strain and thickness of each i th layer, respectively, and a_i is the lattice parameter of i th layer.

TABLE I. Tabulated AFM data from samples in Fig. 2 including dot density, defect density, and dot size for a single layer, three-stack, and five-stack active region with and without GaP SC layers.

		Dot density (cm^{-2})	Defect density (cm^{-2})	Dot diameter (nm)	Dot height (nm)
Single layer	---	5.4×10^{10}	4.0×10^8	32	5.5
Three-stack layer	Without GaP	4.8×10^{10}	9.0×10^8	36	5.9
	With GaP	5.1×10^{10}	6.0×10^8	31	6.0
Five-stack layer	Without GaP	2.8×10^{10}	2.1×10^9	42	7.3
	With GaP	4.9×10^{10}	6.5×10^8	35	7.5

Figures 2(a)–2(d) shows AFM images ($2\ \mu\text{m} \times 2\ \mu\text{m}$) of the surface QD layer atop a (a), (b) three-stack and (c), (d) five-stack active region both with and without 4 ML GaP layers. There are several competing effects that control the QD formation when strain, strain compensation, and defect formation are present. Complete analysis of the strain fields and their effects on nucleation are underway. In this text, we comment on the general trends elucidated in Table I. With increased stacking, the QD density reduces and defect density, QD height, and QD diameter increase. The deleterious effects of stacking are reduced by the introduction of SC layers.

In more detail, the QD density remains constant at $\sim 5 \times 10^{10}$ QDs/ cm^2 as the stacking is increased if SC is incorporated. Without SC, overlapping vertically propagating strain fields likely control the QD nucleation and reduce QD density. As QD density reduces for samples without SC, the defect density increases. The five-stack sample, (c) without SC, has a high defect density of $2.1 \times 10^9 / \text{cm}^2$ and surface undulations. With SC, the defect density remains in the $10^8 / \text{cm}^2$ regime. Increased stacking also causes larger QDs in both width and height, compared to a single QD layer. The diameter increases $\sim 30\%$ for the samples without SC due to a reduced wetting layer thickness (more material in the QDs) and only $\sim 10\%$ with SC. The height increases $\sim 35\%$ both with and without SC.

Room-temperature PL is shown in Figs. 3(a) and 3(b) from four samples (one stack to four stack) with SC and without SC, respectively. Two different peaks are evident in each spectrum. The peak at $1.6\ \mu\text{m}$ is emitted by surface QDs and the shorter wavelength at $1.3\ \mu\text{m}$ is emitted from the capped QD region. The electron-hole pairs are mainly generated in the GaAs buffer layer since the GaAs barriers between the QD actives are very thin. In both types of samples (with and without SC) the relative intensity of the uncapped QDs to the capped QDs reduces with additional stacks as more of the carriers are captured by capped QDs. In Fig. 3(a), the PL intensity increases linearly with each additional QD stack indicating that the number of nonradiative recombination sites does not increase dramatically with stacking. The redshift in the PL peak position with an increased number of stack layers is attributed to an increase in QD size as observed in AFM. In Fig. 3(b), the intensity increases from a one stack to a three stack, then begins to reduce as the fourth stack is added. The intensity from the single QD stack is fairly low because carriers readily thermalize to the lower energy level of the surface QDs where they recombine radiatively at the $1.6\ \mu\text{m}$ wavelength.¹⁷

Finally, we demonstrate lasers that utilize a three-stack InAs QD active with 4 ML GaP embedded in a GaAs matrix. Figure 4 shows the RT lasing characteristics under pulsed conditions (10% duty cycle). The light versus current curve

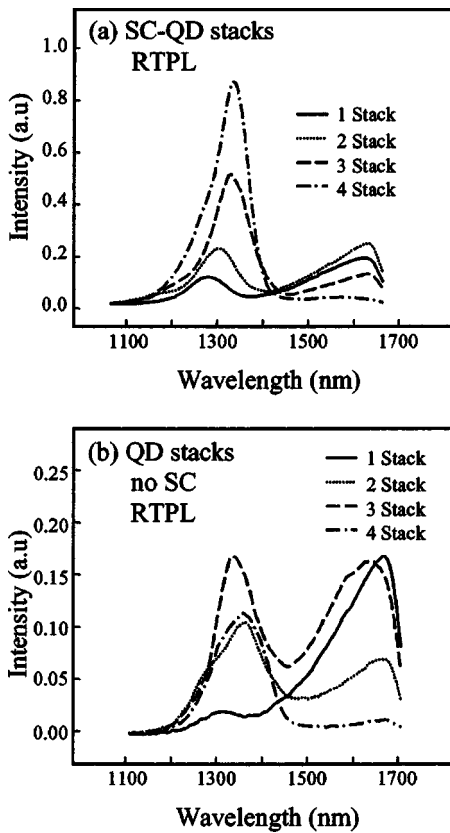


FIG. 3. RTPL spectra comparing single to four-stack QD active regions (a) with SC and (b) without SC layers.

indicates $J_{th}=550 \text{ A/cm}^2$ and the inset shows a multimode lasing spectrum centered at $\lambda=1.249 \mu\text{m}$. The broad area laser dimensions are $50 \mu\text{m} \times 2 \text{ mm}$. High reflectivity coatings (three pairs $\text{Si}/\text{Al}_2\text{O}_3$) are applied by a sputtering technique to both facets. The devices do not lase on the ground state with uncoated facets due to insufficient gain. This al-

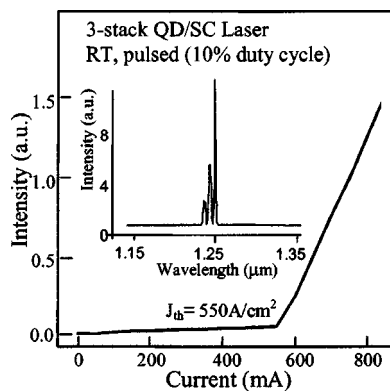


FIG. 4. $L-I$ characteristic and lasing spectra for a three-stack QD laser with 4 ML GaP SC layers.

lows us to place upper and lower boundaries on the three-stack modal gain. We estimate three-stack modal gain to be about 8 cm^{-1} , based on internal loss of about 5 cm^{-1} for MOCVD grown QD laser.^{4,5} We observe a 45 nm blueshift of the lasing peak compared to the RTPL spectra [Fig. 3(a)] which indicates saturation of the larger QDs at high injection current such that lasing transitions originate from smaller QDs.^{16,18} The blueshift in lasing spectra should be suppressed with an increased number of QD stacks.

In conclusion, the GaP SC layer can be used as an important parameter especially for multiple QD-stack systems for extended wavelength lasing where the strain is a very critical issue. The manuscript describes and analyzes the effect of GaP tensile layers embedded in a GaAs matrix to compensate compressive strain in stacked InAs quantum dot (QD) active regions. The optimized GaP thickness is $\sim 4 \text{ MLs}$ and results in a 36% reduction of compressive strain in our device structure. Atomic force microscope images, room-temperature photoluminescence, and x-ray diffraction confirm that strain compensation improves both structural and optical device properties. Room-temperature ground-state lasing at $\lambda=1.249 \mu\text{m}$, $J_{th}=550 \text{ A/cm}^2$ has been demonstrated.

¹A. Stintz, G. T. Liu, H. Li, L. F. Lester, and K. J. Malloy, *IEEE Photonics Technol. Lett.* **12**, 591 (2000).

²O. B. Shchekin and D. G. Deppe, *Appl. Phys. Lett.* **80**, 3277 (2002).

³X. Huang, A. Stintz, H. Li, L. F. Lester, J. Cheng, and K. J. Malloy, *Appl. Phys. Lett.* **78**, 2825 (2001).

⁴S. M. Kim, Y. Wang, M. Keever, and J. S. Harris, *IEEE Photonics Technol. Lett.* **16**, 377 (2004).

⁵I. N. Kaiander, R. L. Sellin, T. Kettler, N. N. Ledentsov, D. Bimberg, N. D. Zakhorov, and P. Werner, *Appl. Phys. Lett.* **84**, 1024 (2004).

⁶J. Tatebayashi, Y. Arakawa, N. Hatori, H. Ebe, M. Sugawara, H. Sudo, and A. Kuramata, *Appl. Phys. Lett.* **85**, 1024 (2004).

⁷A. A. El-Emawy, S. Birudavolu, P. S. Wong, Y. B. Jiang, H. Xu, S. Huang, and D. L. Huffaker, *J. Appl. Phys.* **93**, 3529 (2003).

⁸N. N. Ledentsov, M. V. Maximov, D. Bimberg, T. Maka, C. M. Sotomayor Torres, I. V. Kochnev, I. L. Krestnikov, V. M. Lantratov, N. A. Cherkashin, and Yu. M. Musikhin, *Semicond. Sci. Technol.* **15**, 604 (2000).

⁹B. I. Miller, U. Koren, M. G. Young, and M. D. Chien, *Appl. Phys. Lett.* **58**, 1952 (1991).

¹⁰G. Zhang and A. Ovtchinnikov, *Appl. Phys. Lett.* **62**, 1644 (1993).

¹¹N. Nuntawong, S. Birudavolu, C. P. Hains, S. Huang, H. Xu, and D. L. Huffaker, *Appl. Phys. Lett.* **85**, 3050 (2004).

¹²P. Lever, H. H. Tan, and C. Jagadish, *J. Appl. Phys.* **95**, 5710 (2004).

¹³X. Q. Zhang, S. Ganapathy, H. Kumano, K. Uesugi, and I. Suemune, *J. Appl. Phys.* **92**, 6813 (2002).

¹⁴X. Q. Zhang, S. Ganapathy, I. Suemune, H. Kumano, K. Uesugi, Y. Nabetani, and T. Matsumoto, *Appl. Phys. Lett.* **83**, 4524 (2003).

¹⁵M. Mesrine, J. Massies, E. Vanelle, N. Grandjean, and C. Deparis, *Appl. Phys. Lett.* **71**, 3552 (1997).

¹⁶R. People and J. C. Bean, *Appl. Phys. Lett.* **47**, 322 (1985).

¹⁷K. Shiramine, S. Muto, T. Shibayama, H. Takahashi, T. Kozaki, S. Sato, Y. Nakata, and N. Yokoyama, *J. Vac. Sci. Technol. B* **21**, 2054 (2003).

¹⁸G. S. Solomon, M. C. Larson, and J. S. Harris, *Appl. Phys. Lett.* **69**, 1897 (1996).